

Bistability and hysteresis in self-assembling micelle systems: phenomenology and deterministic dynamics

R. Ball^{*a} and A. D. J. Haymet^b

^a Department of Theoretical Physics, Australian National University, Canberra, ACT 0200, Australia. E-mail: Rowena.Ball.anu.edu.au

^b Department of Chemistry, University of Houston, Houston, TX 77204, USA

Received 21st May 2001, Accepted 23rd August 2001

First published as an Advance Article on the web 11th October 2001

We analyse a simplified dynamical model that emulates the overall process of self-assembly of amphiphilic molecules into micelles under non-equilibrium conditions. The study is motivated by a review of experimental evidence in the literature for the occurrence of bistability and hysteresis in diverse self-assembling molecular systems. Singularity theory conditions and classifications for bifurcations are used to map the bifurcation structure of the model. The analysis predicts that self-assembling micellar systems may exhibit bistability and hysteresis. It also provides a map of the boundaries of multiplicity, which effectively defines the role of the model parameters in producing and maintaining hysteretic behaviour. Anomalous hysteresis is identified in the model, and the implications of this for the design and engineering of self-assembling systems are discussed with reference to experimental data for the autocatalytic production of caprylate micelles. We also investigate the occurrence of oscillatory behaviour. In a model having a single outflow or sink rate f for amphiphile and micelles it is shown that Hopf bifurcations to limit cycles are effectively trapped at $f = -\infty$. In a more realistic model, where the sink rates for amphiphile and micelles are finitely coupled or uncoupled, limit cycles can move into the physical parameter space and interact with the hysteretic region. The results of this study suggest that the hysteresis loop in non-equilibrium self-assembling systems could be used as a switch.

1 Introduction

Micelle formation from amphiphilic monomers in solution is often found to be a highly nonlinear kinetic process, in experiments and simulations,^{1–6} that is indicative of a co-operative or autocatalytic mechanism. Under non-equilibrium conditions steady-state multiplicity, with accompanying hysteresis, is likely to be endemic to such systems. In this work we apply singularity and stability analyses^{7,8} to enumerate and interpret the bifurcations occurring in a simple 2-dimensional dynamical model that emulates the overall process of micelle formation in a non-equilibrium system. We find that hysteretic jumps between associated and dissociated states are controllable in principle, by varying the relative rates of supply and removal of monomer, thus giving us a molecular system engineering tool of potentially great power.

Steady-state multiplicity and hysteresis are known to occur in many different physico-chemical systems, although the associated non-equilibrium properties and processes are less well-understood than the singular equilibrium state. Hysteretic and oscillatory transitions to self-ignited states have been well-documented in thermokinetic systems, where the strongly non-linear behaviour is due to the temperature dependence of reaction rates competing with linear cooling processes (*e.g.* ref. 9 and 10). Qualitatively similar dynamical behaviour has also been observed in some isothermal reaction systems that are more well-known for displaying complex and chaotic oscillations and spatial patterns (*e.g.* the BZ reaction in closed¹¹ and open¹² systems).

There is also experimental evidence for the occurrence of bistable states in associating molecular systems, such as solutions of amphiphiles that form micelles and in more specific macromolecular interactions. Examples are abundant,

although rather scattered, in the literature and in section 2 we review some representative cases.

The rest of the paper is organised as follows. In section 3 we outline a kinetic model for micelle formation, based on existing models in the literature, incorporating nonlinear feedback and competing rate processes that introduce the potential for bistability. The detailed bifurcation analysis of this model is carried out in section 4. Hysteresis with respect to the outflow or sink rate is found to be anomalous, in that the bifurcation curve has an “in-phase” *iso* branch and an “out-of-phase” *anti* branch. The implications for design and control of self-assembling systems are discussed. The extent of multiplicity over the parameter space is defined graphically. Section 5 explores the occurrence of limit cycles in a more realistic system containing finitely coupled or uncoupled sink terms that may include both specific chemical sink rates and an outflow rate. The rationale is that, in the design and operation of hysteretic self-assembling systems, we need to know how oscillatory behaviour may interfere. The conclusions are summarized in section 6.

2 Evidence for bistability in associating molecular systems

In retrospect, some significant experiments that relate to the current topic were reported by Ball *et al.* in ref. 13. In that work, in which the charge-transfer interactions of drug molecules were studied, the conductivity of aqueous iodine solution was measured as a solution of amiodarone¹⁴ was added. In the reverse experiment the conductivity of amiodarone solution was followed as iodine solution was added. The experiments were carried out quasistatically, in that the rapid transient that occurred at each dose of titrant was allowed to

subside prior to recording the conductivity and adding the next dose of titrant. (The approach to equilibrium after each initial transient spike was relatively slow, so that at the time of adding each dose of titrant the system was effectively in a non-equilibrium, stationary state.) The data and interpolated curves of solution conductivity against mole fraction of amiodarone are reproduced in Fig. 1.

Here there is clear evidence of a bistable system that was not discussed in the original work: the forward and reverse curves do not coincide. Micellar association of the amphiphile occurs at a mole fraction of ~ 0.15 in the forward titration, but in the reverse titration the monomer is evidently released from the micelles that are initially present. (Hysteretic transitions between the two states may not be observed in this type of experiment because the system is relaxing slowly towards thermodynamic equilibrium as the experiment proceeds, *i.e.*, it was not designed as a true non-equilibrium steady-state experiment.)

The first experiments to demonstrate that a micelle-forming system could exhibit bistability in externally controllable non-equilibrium conditions were reported in ref. 15. In that work, the alkaline hydrolysis of ethyl caprylate to form caprylate micelles was carried out in a continuous stirred tank reactor (CSTR). Hysteresis of the ethyl caprylate concentration with respect to the residence time was measured. In section 3.3 we shall use the CSTR model as a paradigm for a non-equilibrium condition that may include chemical sinks as well as a through-flow or outflow rate. The crucial point to remember is that hysteresis is unequivocally a non-equilibrium phenomenon.

Hysteresis with respect to temperature as the control parameter has been characterized in ganglioside micellar association.^{16–20} Since gangliosides are involved in the mechanism of information flow through neuronal cell membranes,²¹ it is believed to have a signalling function. The interconversion is between two different aggregational states of the gangliosides, rather than between the free monomer and micellar states. Another case was described in ref. 22, where hysteresis was seen between two conformations of self-assembled diblock copolymer micelles.

Highly specific macromolecular associations can also exhibit bistability. The formation and dissociation of van der Waals complexes of a specific antigen–antibody complex was shown to be hysteretic with respect to the surface tension of the aqueous medium.²³ The hysteresis was attributed to a slow expulsion of solvent between the antibody active site and the antigenic determinant after the complex is formed, which strengthens the Van der Waals interactions.

Hysteretic control is also known to be important in live biological systems. Experimentally characterized examples are

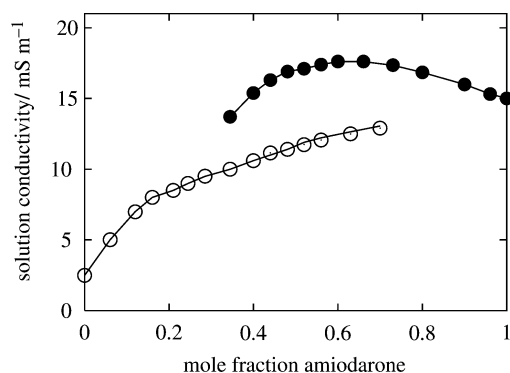


Fig. 1 The conductivity titration experiment from ref. 13: solution conductivity against mole fraction of the drug amiodarone. White circles: increasing mole fraction of amiodarone (“forward” experiment). Black circles: increasing mole fraction of iodine (“reverse” experiment). Redrawn from original data.

the control of current–voltage relationships across ion channels,²⁴ neural control of lung function *via* changes in surfactant surface tension,²⁵ and the activity of antifreeze proteins in lowering the freezing point in cells.^{26,27} Kinetic modelling studies have supported experimental evidence for the role of hysteresis *in vivo*. Results in ref. 28 suggest that it is important in controlling the aggregation states of the disease-causing prion protein, and the modelling work in ref. 29 strongly corroborates evidence that the activity of an essential enzyme in cell-division is exquisitely controlled by hysteretic jumps with respect to the level of a co-factor. Models for cell-signalling feedback loops that control processes such as oocyte maturation have been shown to exhibit bistability,^{30,31} and it has been suggested that such bistable processes have evolved as a sensitive control mechanism.

The latter examples are very reassuring: if hysteresis exists at all in biological systems, then one might *expect* that evolution would have long since found ways of taking advantage of it as a control mechanism. If indeed nature thought of it first, the idea of engineering the hysteresis loop to control the dynamical behaviour of associating molecular systems is well-founded. However, hysteretic behaviour is in general not well understood, and is often regarded as idiopathic, artifactual, or having nuisance or curiosity value. In the approach taken in this work it is viewed not as a pathological phenomenon but as a design and control tool in molecular engineering applications (or nanotechnology). Since a hysteresis loop is effectively a switch, investigations into the causes and consequences of hysteretic bistability may provide new mechanisms for chemical information transfer. In particular, we believe hysteresis may be used in the design of tunable drug delivery systems, in the sensitive control of anaesthetic action, and in the operation of molecular switches in bioimmunoassay systems.

3 A kinetic model for micelle formation

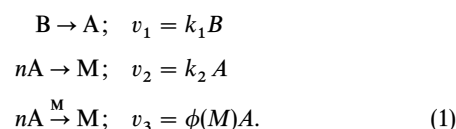
3.1 Non-equilibrium states in self-assembling systems

Free monomeric amphiphiles in solution may aggregate rapidly into clusters when one or more system parameters (such as ionic strength, monomer concentration, surface tension, or temperature) is changed, in a process that has some similarities to phase transitions. Whichever parameter is actually varied in experiments, the onset of rapid uncontrollable aggregation is most usually related to a critical concentration of free monomer called the *critical micelle concentration*.

The critical micelle concentration is by definition singular, an equilibrium property. In this work we shall refer to the analogous non-equilibrium critical points as *critical assembly/disassembly points*. As intimated above the existence of bistability in assembling systems immediately suggests the possibility of engineering hysteretic systems, to control the positions of the critical assembly/disassembly points in state and parameter space and the shape and slope of the bifurcation curves. Some possible configurations of the hysteresis loop are sketched in Fig. 2.

3.2 Power-law autocatalysis provides a feedback mechanism

A simplified kinetic scheme for micelle formation may be written as follows:



This scheme describes first-order decay of an inactive precursor B into the active amphiphile A, which may assemble into

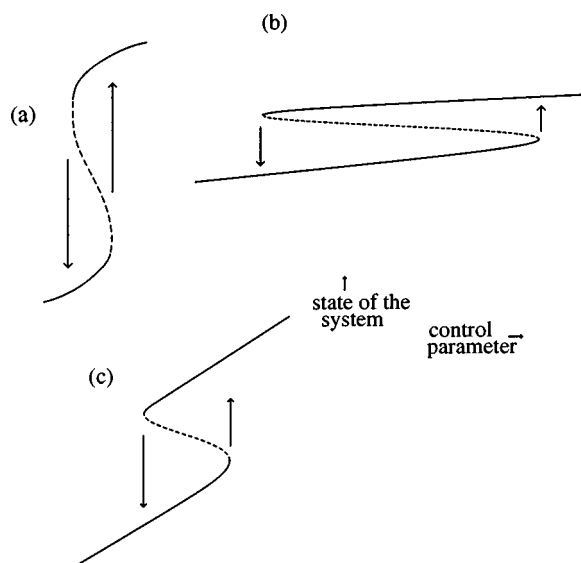
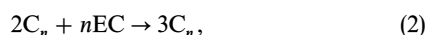


Fig. 2 We would like to engineer molecular switching systems that display the dynamical properties indicated in these sketches. (a) Tall thin hysteresis—dramatic jumps in the state variable but sensitive to changes in the control parameter. (b) Short fat hysteresis—a lot of play in the system over a broad range of the control parameter. (c) Very sloping hysteresis—significant continuous changes before the jumps occur.

micelles M in two ways. The italicized symbols represent concentrations of the species, v_1 , v_2 and v_3 are the rates of each process, and n is the nominal monomer number. The second step is a slow, uncatalysed process occurring with an effective first-order rate constant k_2 . In the third step the micelles may catalyse their own formation. The autocatalytic rate constant $k_3 = \phi(M)$ is a nonlinear function ϕ of the micelle concentration, specified below.

It should be emphasized that this scheme is intended purely as a phenomenological description. No assumptions concerning molecularity or stoichiometry or detailed reaction mechanisms are implied, nor does this model say anything about the size distribution of the micelles. In this sense it is a crude description of the gross dynamics of micellization, making no reference to molecular-scale or step-wise processes. Nevertheless, schemes similar to (1) have been used very successfully to model and predict micelle formation. In ref. 2 it was found that computed trajectories of a clock reaction model that included the autocatalytic step



where C_n represents the caprylate micelles and EC the substrate, agreed well with the experimental time–evolution data. A more detailed (although still macroscopic) kinetic scheme for the ethyl caprylate/caprylate/micelle system was proposed and validated experimentally by Buhse *et al.*,⁴ in which the nonlinearity responsible for the autocatalysis arises from reversible phase-transfer between organic and aqueous phases. In both of these works the authors found the formal termolecular step conceptually problematic, since as written in (2) it implies that autocatalysis requires two micelles to communicate with each other and with enough monomers to form three micelles—certainly a difficult physical situation to picture. We have taken a lesson from the biochemists and simply written the autocatalytic step using the feedback notation as indicated for rate enhancement by the reaction product. In this way we are not constrained by spurious notational stoichiometry and we are free to choose the nonlinear function $\phi(M)$ empirically or according to more fundamental considerations.

In this work we shall follow ref. 2 and choose $\phi(M) = k_3 M^2$ without proposing a microscopic or mechanistic interpreta-

tion of the power-law dependence of the autocatalytic rate constant. This is often called *cubic autocatalysis* because the catalytic rate equation is third-order overall. Reaction schemes similar to (1) have been studied extensively from the 1970s, when a prototype (the *brusselator*) was first proposed by the Brussels school of Prigogine and co-workers³² as a model for oscillating reactions. Models derived from similar isothermal autocatalytic schemes were later analysed using bifurcation theory.^{33–38} With this choice of the autocatalytic function $\phi(M)$ the reaction scheme (1) gives rise to the following dynamical system, written in dimensionless form:

$$\frac{dx}{d\tau} = \mu(b_0 - x - y) - rx - xy^2 \quad (3)$$

$$\frac{dy}{d\tau} = rx - xy^2, \quad (4)$$

where x , y and b are the dimensionless concentrations of active free amphiphile (A), micelles (M) and precursor (B) respectively. Eqn. (3) and (4) are derived in Appendix A and the dimensionless variables and parameters in these and subsequent equations are defined in Table 1, Appendix B.

This system has no non-trivial steady states. It is very similar to that used by Billingham and Coveney,² for which asymptotic analysis gave induction times for the onset of micellization. However, in order to explain experimental observations of state bistability in self-assembling systems it is clear that we need to introduce a non-equilibrium or flux condition that permits the existence of non-trivial stationary solutions.

A number of other kinetic models for the self-assembly of micelles have been proposed. Some (*e.g.* ref. 39) rely on an equilibrium thermodynamic formalism and are therefore outside the scope of this work. Others, such as those based on generalized Becker–Döring equations,^{3,40} aim to reproduce quantitatively the induction time to the rapid onset of aggregation and the critical micelle concentration. However, the non-equilibrium condition that is required for bistability is not built into those models.

3.3 The CSTR formalism provides a non-equilibrium stationary state condition

From chemical engineering we borrow the concept of the CSTR (continuous stirred tank reactor) as a simple paradigm that models the essential features of reacting, nonequilibrium liquid-phase systems. The feedstream to a reacting cell of volume V delivers reactants at a constant volumetric flow rate F . Inside the cell spatial gradients are negligible (it is well-stirred), conversion of the reactants occurs at a rate that depends on the balance between the reaction rate and the residence time V/F , and products + reactants are removed in the effluent. Isothermal operation is ensured by thermostating the cell.

Although the well-stirred assumption is an idealization that may not be justified in situations where transport processes govern dynamical behaviour, the CSTR has many advantages as a model for studying non-equilibrium processes, both in the living cell and in the laboratory. The capacity for steady-state operation is crucial here, as is the putative flow rate F which can also describe physico-chemical mechanisms of reactant supply and product removal. The CSTR is thus a very convenient construct for representing any situation where there is a constant supply of reactant from an infinite reservoir, a constant rate of removal of reactant and products, and where diffusion can be neglected. Last, but not least, the CSTR is experimentally accessible.¹⁵

Using the CSTR formalism we can impose a non-equilibrium condition on the reaction sequence in (1), which

yields the following dynamical system:

$$\frac{dx}{d\tau} = \mu - xy^2 - x(r + f) \quad (5)$$

$$\frac{dy}{d\tau} = rx + xy^2 - fy \quad (6)$$

$$b(0) = 1, \quad x(0) = 0, \quad y(0) = 0. \quad (7)$$

This is the system we shall work with. Eqn. (5)–(7) are derived in Appendix A and the dimensionless groups are defined in Table 1, Appendix B.

4 The bifurcation analysis

We begin by setting the time derivatives in eqn. (5) and (6) to zero. Of the three parameters, f is a control parameter, representing the flux rate through the system, and μ and r are intrinsic or design parameters, not variable after the reaction system and conditions are chosen. It is therefore most appropriate to select f as the principal bifurcation parameter and to regard the state variable as an implicit function of f . The choice of state variable will therefore govern the shape of the bifurcation diagram, and we shall consider each in turn.

With y_s , the steady-state concentration of micelles, as the state variable, the bifurcation equation is

$$G = \frac{\mu}{r + y_s^2 + f} (r + y_s^2) - fy_s = 0. \quad (8)$$

The general defining conditions for the hysteresis variety⁷

$$G = G_\xi = G_{\xi\xi} = 0, \quad G_{\xi\xi\xi} \neq 0, \quad G_{\xi\lambda} \neq 0, \quad (9)$$

where ξ is the state variable (y or x), λ represents the selected bifurcation parameter, and the subscripts indicate partial derivatives, evaluated with respect to y_s and f , are diagnostic of threefold multiplicity and hysteresis:

$$G_y = \frac{2\mu y_s f}{(y_s^2 + r + f)^2} - f = 0 \quad (10)$$

$$G_{yy} = \frac{2\mu f(f + r - 3y_s^2)}{(y_s^2 + r + f)^3} = 0 \quad (11)$$

$$G_{yyy} = \frac{-24\mu f y_s (f + r + 3y_s^2)}{(y_s^2 + r + f)^4} < 0 \quad (12)$$

$$G_f = -\frac{\mu(r + y_s^2)}{(r + y_s^2 + f)^2} - y_s < 0. \quad (13)$$

The stability of solutions to eqn. (8) and the quality of the hysteresis are shown in the bifurcation diagram of Fig. 3(a). (Note: In order to provide reassurance that we are working in an appropriate region of the parameter space the values of the intrinsic parameters μ and r were calculated using the numerical values of the rate constants given in ref. 2 for amphiphile formation and non-catalysed and catalysed formation of

caprylate micelles.) On both the upper and lower stable branches in Fig. 3(a) the steady state concentration of micelles (y_s) decreases as the flow-rate f increases. This is to be expected: interpreted as an inverse residence time, an increase in f means there is less time for micelles to form.

With x_s , the steady-state concentration of free amphiphile, as the state variable, the situation appears to change radically. The conditions (9) evaluate as follows:

$$G = x_s \left(\frac{\mu}{f} - x_s \right)^2 + rx_s - f \left(\frac{\mu}{f} - x_s \right) = 0 \quad (14)$$

$$G_x = \left(\frac{\mu}{f} - x_s \right)^2 - 2x_s \left(\frac{\mu}{f} - x_s \right) + r + f = 0 \quad (15)$$

$$G_{xx} = 2 \left(3x_s - \frac{2\mu}{f} \right) = 0 \quad (16)$$

$$G_{xxx} = 6 \neq 0 \quad (17)$$

$$G_f = \left(\frac{2\mu x_s}{f^2} \right) \left(x_s - \frac{\mu}{f} \right) + x_s \neq 0 \quad (18)$$

for $G = G_x = G_{xx} = 0$.

The bifurcation curve in Fig. 3(b) shows the stability of solutions and the shape of the hysteresis loop. Here the concentration of free amphiphile x_s may decrease or increase with f , depending on where the system is initially placed on the bifurcation curve. On the upper stable branch in Fig. 3(b) the amphiphile concentration decreases with increasing f , but on the lower branch the amphiphile concentration increases with increasing f . By reference to Fig. 3(c), the projection of the bifurcation curve onto the x_s - y_s plane, and considering Fig. 3(a) and (b) together it can be seen that there is a range of steady states across which both free amphiphile x_s and micelles y_s may accumulate.

This result seems counter-intuitive, or at least in need of physical interpretation. Let us pause in the bifurcation analysis and temporarily set aside the algebra. What sort of qualitative behaviour do we expect to find in this system?

The amphiphile accumulates due to decay of the precursor but is removed by micelle formation and by flow out of the reacting volume. Micelles accumulate autocatalytically and non-catalytically and are also removed in the outflow. We would expect that whenever micelles are accumulating, the amphiphile is concurrently being depleted; or conversely, when fewer micelles are available (due to more rapid outflow) to participate in autocatalysis, amphiphile would accumulate. Indeed, this scenario occurs on the upper stable sections of the curves in Fig. 3(a) and (c), which correspond to the lower stable curve section in Fig. 3(b). To avoid confusion, we shall call this branch the *anti* branch. At the right-hand limit point the concentration of amphiphile x_s jumps to the upper stable section of the curve while that of micelles y_s jumps to the lower stable curve section. This branch we shall call the *iso* branch. Now, however, we have the anomalous effect noted above: both concentrations change in the *same* direction as we traverse the *iso* branch, until the hysteretic jump at the

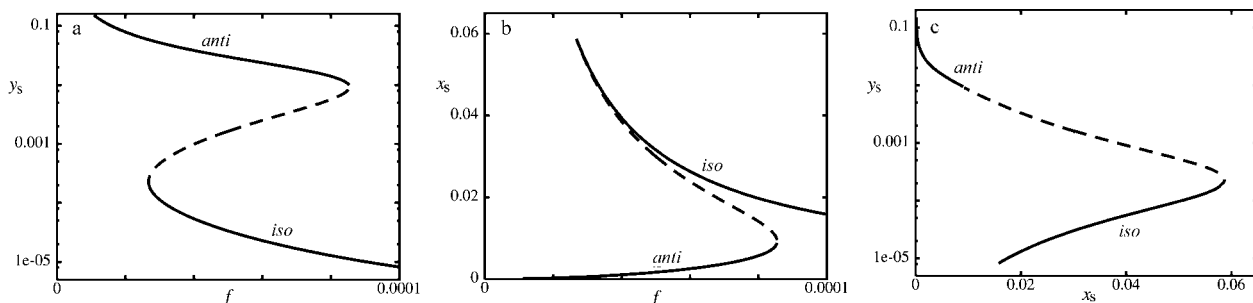


Fig. 3 Steady state solutions of eqn. (8) in (a) the y_s - f plane, (b) the x_s - f plane, and (c) the x_s - y_s - f space, projected onto the x_s - y_s plane. $\mu = 1.58 \times 10^{-6}$, $r = 5.18 \times 10^{-8}$. Solid lines represent stable solutions, dashed lines unstable solutions.

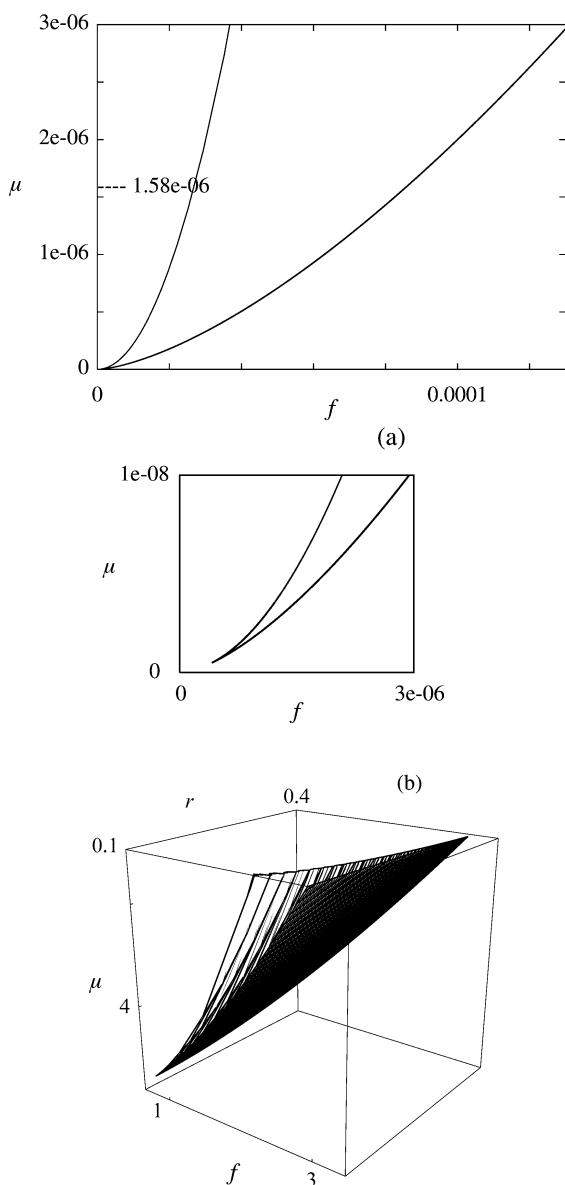


Fig. 4 (a) Loci of limit points in the f - μ plane for $r = 5.18 \times 10^{-8}$. The magnification of the lower left-hand portion shows the cusp at the onset of hysteretic multiplicity. (b) The steady-state limit point surface of eqn. (5) and (6).

left-hand limit point occurs. Along this branch decay of the precursor to form the active amphiphile occurs faster than the micelles can remove the amphiphile.

The geometrical reason for this in-phase mode is obvious when eqn. (13) and (18) are compared— G_f cannot equal zero for any physical values of the parameters when y_s is the steady-state variable, but G_f can equal zero along the steady-state curve when x_s is the steady-state variable. (At the parameter values we have used in these calculations the points of vertical and horizontal tangency on Fig. 3(b) are very close, so there appears to be a degenerate cusp there. However, there is no degenerate point, as eqn. (14)–(18) show.)

The implications for control and engineering of self-assembling systems are clear. If it is desired to run the system under “low amphiphile” conditions (perhaps the amphiphile may be toxic) then maintenance on the *anti* branch is preferable. On the other hand, if a high enough concentration of amphiphile is required to justify operation on the *iso* branch we should be aware that downwards drift or tuning of f can further increase the concentration of amphiphile and also increase that of the micelles.

4.1 The extent of multiplicity

In the design and engineering of self-assembling systems the extent of multiplicity over the parameter space is just as important as the shape of the hysteresis loop. To obtain a map of the boundaries of multiplicity the limit points in Fig. 3(a) and (b) can be tracked by varying another parameter, selected as μ . The loci of limit points are shown projected onto the f - μ parameter plane in Fig. 4(a). Indicated is the constant- μ slice from which the bifurcation diagrams of Fig. 3(a) and (b) may be reconstructed. These curves can be obtained analytically by evaluating the limit-point defining conditions

$$G = G_\xi = 0, \quad G_{\xi\xi} \neq 0, \quad G_\lambda \neq 0 \quad (19)$$

(Eqn. (8), (10), (11) and (13)) and rearranging to the following explicit expressions parametrized by y_s :

$$f = \frac{(y_s^2 + r)^2}{(y_s^2 - r)}, \quad \mu = \frac{(y_s^2 + r)2y_s^3}{(y_s^2 - r)^2}. \quad (20)$$

For the given value of r a target state of the system can be selected from Fig. 4(a). When r is also allowed to vary, the cusp at the onset of multiplicity may be unfolded to a curve in the 3-dimensional parameter space by rearranging eqn. (8), (10) and (11):

$$f = 8y_s^2/3, \quad \mu = 8y_s^3, \quad r = y_s^2/3. \quad (21)$$

This curve is the watershed of a surface of limit points, of which Fig. 4(a) is a slice. A section of the limit point surface is illustrated in Fig. 4(b). The seam of codimension 1 points defined by eqn. (22) joins the two sides of the surface. Since there are no higher-order singularities and no more parameters in the model this surface is absolute in the steady-state solution space of eqn. (5) and (6): it cannot scale, translate, rotate, or undergo topological deformations.

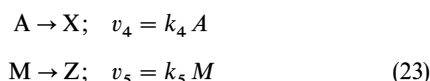
5 Chemical sources and sinks may induce limit cycles

For a two-dimensional dynamical system the conditions for non-degenerate Hopf bifurcations to limit cycles⁴¹ may be expressed as

$$G = \text{tr } J = 0, \quad \det J > 0, \quad \frac{d(\text{tr } J)}{d\lambda} \neq 0, \quad \rho_2 \neq 0, \quad (22)$$

where $\text{tr } J$ and $\det J$ are the trace and determinant of the Jacobian matrix of the differential coefficients of the linearization, and ρ_2 determines the stability of the emergent limit cycle. Evaluation of the conditions (23) for eqn. (5) and (6) confirms that Hopf bifurcations are absent: we find that $G = \text{tr } J = 0$ only for non-physical values of f . The absence of Hopf bifurcations does not in general forbid the existence of oscillations. In this case, it can be proved using Dulac's criterion⁴² that eqn. (5) and (6) cannot have oscillatory behaviour arising from any source for $f > 0$. The proof is technical, and we do not present it here.

However, as discussed above, the nominal flowrate in the CSTR formalism can also represent chemical sources or sinks for reactants or products. We have already one chemical source in the system—decay of the precursor to active amphiphile. Chemical sinks for the amphiphile and the micelles may be represented by the following steps additional to the sequence (1):



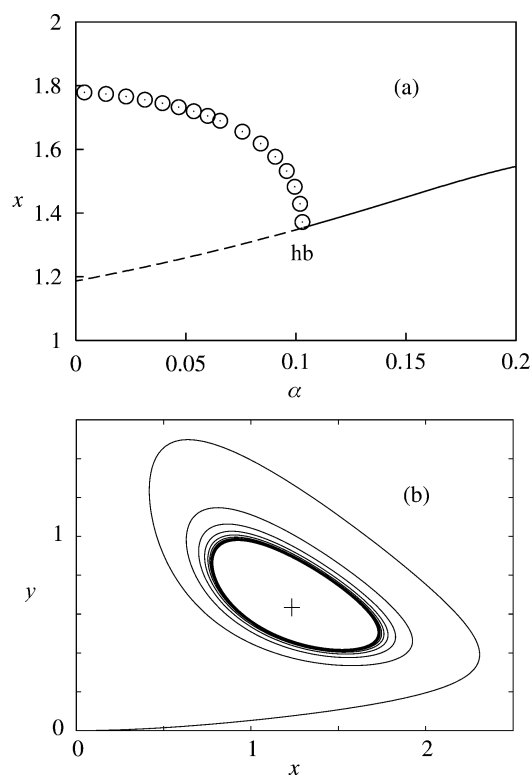


Fig. 5 Oscillatory solutions of eqn. (25), $\eta = 1.0$, $\mu = 0.7$, $r = 0.1$. (a) A bifurcation diagram. hb labels a Hopf bifurcation, open circles mark the maximum x -amplitude of the limit cycles. (b) A phase portrait, $\alpha = 0.05$.

The combined reaction scheme (1) and (23) may be written as the following dissipative dynamical system:

$$\frac{dx}{d\tau} = \mu - xy^2 - x(r + \alpha) \quad (24)$$

$$\frac{dy}{d\tau} = rx + xy^2 - \eta y. \quad (25)$$

Initial conditions are not specified: they must be arbitrary because the introduction of two separate sink terms effectively breaks the conservation condition that permits formal elimination of one state variable. This system is treated as planar by assuming constant concentration of the precursor.

More generally, the rate coefficients α and η may represent combined quantities that include a common flow-rate component as well as separate chemical sink-rates for each species.

Although the steady-state bifurcation structure of eqn. (24) and (25) is formally identical to that of eqn. (5) and (6), the stability properties of the solutions allow for Hopf bifurcations to limit cycles. Fig. 5(a) shows a steady-state bifurcation curve for eqn. (24) and (25), with x as the state variable and α as the bifurcation parameter. The Hopf bifurcation *hb* and the maximum amplitude trace of the branch of stable limit cycles are indicated. Obviously the region of parameter space here is well outside the range of multiplicity. The phase portrait in Fig. 5(b), computed for a value of α selected from the unstable portion of the curve in (a), shows a trajectory that spirals into a limit cycle.

5.1 Coupling of sink-rates introduces Hopf bifurcations

An implication of the preceding analysis is that Hopf bifurcations are forbidden when α is identically equal to η ($=f$) and spring into being, fully formed, when $\alpha \neq \eta$. Such a discontinuity is both theoretically and practically problematic. When we view α and η as combined chemical sink/flow coefficients

there is no *a priori* reason why $\alpha = \eta$ should be an exceptionally singular condition. In real life a flow system that is designed with a certain amount of controllable hysteresis may also have one or more intrinsic chemical sinks that remove reacting species. It is obviously of interest to be able to evaluate the extent to which chemical sinks may affect operation of the system.

This problem of a spurious singularity occurring at $\alpha = \eta$ with respect to the appearance of Hopf bifurcations may be resolved by explicitly including a continuum coupling formalism between the two sink-rates in eqn. (24) and (25). The simplest way is to write η as a linear function of α :

$$\eta = \frac{\eta^0 + \kappa\alpha}{1 + \kappa} \quad (26)$$

where κ is a constant. The form of this function ensures that when $\kappa = 0$, $\eta = \eta^0$ (full decoupling), and in the limit $1/\kappa \rightarrow 0$ $\eta = \alpha$ (full coupling). A similar function was used in ref. 43 to resolve an anomaly in the steady-state bifurcation structure of the exothermal CSTR problem; here it is used to achieve a smoothly traversible Hopf bifurcation parameter space. Using the function (26), eqn. (25) may be rewritten as

$$\frac{dy}{d\tau} = rx + xy^2 - \frac{\eta^0 + \kappa\alpha}{1 + \kappa} y. \quad (27)$$

We are now working with a more general system comprising eqn. (24) and (27). The origin and fate of the Hopf bifurcations may be followed in the α - μ parameter planes of Fig. 6. The loci of limit points and Hopf bifurcations in the figures have been obtained by evaluating the limit point conditions $G = G_y = 0$ and the Hopf bifurcation equalities in (22) to explicit parametric equations. For the limit-point loci we obtain

$$\alpha = \frac{(y_s^2 + r)^2}{(y_s^2 - r)} \quad (28)$$

$$\mu = \frac{\eta^0 + \kappa\alpha}{1 + \kappa} \frac{2y_s^3}{(y_s^2 - r)^2} \quad (29)$$

and for the Hopf loci

$$\alpha = \frac{\eta^0(y_s^2 - r) - (y_s^2 + r)^2(1 + \kappa)}{y_s^2 + r + 2\kappa r} \quad (30)$$

$$\mu = \left(\frac{\eta^0 + \kappa\alpha}{1 + \kappa} \right)^2 \frac{y_s(y_s^2 - r)}{(y_s^2 + r)^2}. \quad (31)$$

Now it is easy to see that Hopf bifurcations are in fact endemic to the generalized system. In eqn. (30) and (31) when $\kappa = 0$ (zero coupling) we have $\eta = \eta^0$ and $\alpha = \eta^0(y_s^2 - r) - (y_s^2 + r)^2/y_s^2 + r$, $\mu = (\eta^0)^2(y_s(y_s^2 - r))/(y_s^2 + r)^2$. When $\kappa \rightarrow \infty$ eqn. (30) may be rewritten

$$\alpha = \frac{\frac{\eta^0(y_s - r)}{\kappa} - (y_s^2 + r)^2 \left(\frac{1}{\kappa} + 1 \right)}{\frac{y_s^2 + r}{\kappa} + 2r}.$$

In the limit $1/\kappa \rightarrow 0$

$$\alpha = - \frac{(y_s^2 + r)^2}{2r}. \quad (32)$$

In Fig. 6(a) the Hopf bifurcation from Fig. 5 is unfolded using eqn. (30) and (31) with $\kappa = 0$, and the locus is plotted together with the region of multiplicity enclosed by the limit-point loci. It is a very useful diagram because we can see at a glance that multiplicity near the given values of η , r and κ is not likely to be complicated by oscillatory behaviour resulting from Hopf bifurcations, and *vice versa*.

At a larger value of the sink rate η , and still with zero coupling, the Hopf and limit-point loci can interact as shown in

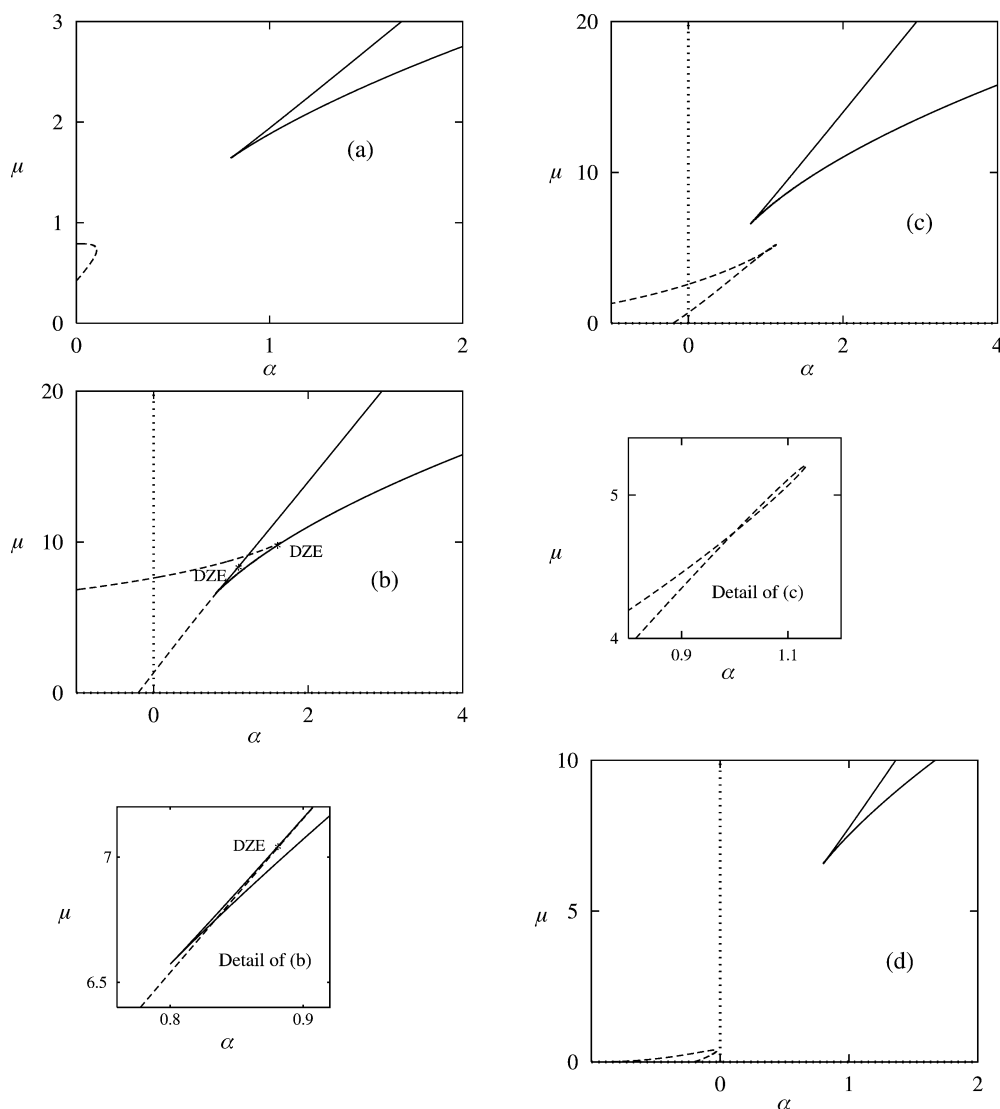


Fig. 6 Loci of limit points (solid lines) and Hopf bifurcations (dashed lines) projected in the α - μ parameter plane, for eqn. (24) and (27). (a) $\eta = 1.0$, $r = 0.1$, $\kappa = 0$. (b) $\eta = 4.0$, $r = 0.1$, $\kappa = 0$. DZE labels double zero eigenvalue points. (c) $\eta = 4.0$, $r = 0.1$, $\kappa = 1$. (d) $\eta = 1.0$, $r = 0.1$, $\kappa = 4.2$.

Fig. 6(b). At the two DZE points of interaction with the limit-point loci the Hopf locus terminates because $\det J = 0$ (see eqn. (22)). More generally, such DZE points occur where the Jacobian has two zero eigenvalues). The other crossings in this diagram are non-local.

The Hopf and limit-point loci for non-zero κ are shown in Fig. 6(c) and (d). (The apparent intersection in (c) is non-local.) These diagrams clearly illustrate where the Hopf bifurcations come from in the generalized system: they are trapped at negative infinity for fully coupled sink terms, and emerge from beyond the physical limit as the degree of coupling decreases.

6 Discussion and conclusions

A dynamical system similar in form to eqn. (24) and (25), and also based on a cubic autocatalytic reaction scheme, was analysed first in ref. 33 and later in ref. 36. The highest order singularity was found to be a winged cusp, for which four parameters are required for a full unfolding. However, the work in ref. 33 and 36 was abstract and general, in that the system they used was not intended to model a specific process.

In the context in which our work is set—the non-equilibrium formation of a bistable micellar system—there are effectively only two physically different, independently controllable (in principle) attributes or quantities: parameters that may be described as input or generation rate coefficients and those that may be described as output or dissipative rate-

coefficients. The former are represented by μ and r and the latter by f , or η and α . Broadly speaking, our system is a coupled juxtaposition of generation and loss rate processes, which inevitably give rise to nonlinear behaviour when they are incommensurate. One of the purposes of nonlinear modelling and analysis is to suggest experiments, and we have therefore chosen to dwell within the parameter space in which experiments could be carried out.

The evidence of micellar bistability in experiments, such as the amiodarone-iodine titration shown in Fig. 1, and in the autocatalytic model that emulates micellization raises the question of how events on molecular time and space scales coarse-grain into the observed cooperativity. This is a big issue, that cannot be resolved on the basis of continuum rate models, but may be tackled by very large computational simulations. On a mass action level it is not difficult to see how nonlinear behaviour arises. From Fig. 6 we can see that oscillatory and jump behaviour occurs when the supply rates (μ and r) and removal or sink rates are significantly mismatched. For example, in Fig. 6(b) oscillations occur in a region where the throughput of monomer is faster than that of micelles. Micelles alternately accumulate, because their loss rate is slow, and are depleted, because insufficient monomer is accumulating to maintain the micelle concentration. On the other hand, a rapid jump to a state of high micellization can occur in a region where monomer accumulates more rapidly than it is removed.

We may summarize the results of this work as follows:

1. The overall process of micelle formation in non-equilibrium conditions may be emulated by a simple low-dimensional autocatalytic model that shows non-trivial stationary states, multiplicity, and hysteresis.

2. The steady-state curves in the hysteretic régime have an *anti* branch, along which the concentrations of amphiphile and micelles vary oppositely, and an *iso* branch, along which the concentrations of amphiphile and micelles vary in the same direction.

3. The hysteresis loop provides a method of switching on and off the association and dissociation of amphiphiles and micelles by appropriate tuning of a parameter, provided the bifurcation behaviour with respect to the parameter is mapped.

4. Limit cycles due to Hopf bifurcations do not occur when the flux term that simulates non-equilibrium conditions represents fully coupled rates of removal of reactants and products. They may occur when there are separate sinks for amphiphiles and micelles.

5. Although the model was presented using a CSTR paradigm to maintain the system away from equilibrium, diverse examples from the literature suggest that physicochemical mechanisms that induce non-equilibrium stationary states often operate in self-assembling systems. The analysis of the model presented in this work stands on its own as a potentially sensitive method of engineering and controlling self-assembling systems. It is also a step towards a mesoscopic or microscopic understanding of intrinsic nonequilibrium mechanisms that may operate in amphiphilic systems.

Acknowledgement

This research was supported by Australian Research Council grant A29530010 (ADJH) and an Australian Research Council Fellowship (RB). Some of this work was completed during a visit by RB to Leeds University, supported under the Australian Academy of Science Scientific Visits to Europe programme. In USA ADJH is supported by Welch Foundation grant E-1429.

Appendix A: Derivation of eqn. (8)–(10)

Mass balances for the system (1) may be written in dimensionless form as follows:

$$\frac{dB}{dt} = -k_1 B + \frac{F}{V} (B_f - B) \quad (33)$$

$$\frac{dA}{dt} = k_1 B - k_2 A - \phi(M)A + \frac{F}{V} (A_f - A) \quad (34)$$

$$\frac{dM}{dt} = k_2 A + \phi(M)A + \frac{F}{V} (M_f - M). \quad (35)$$

Mass conservation may be used to reduce the dimensionality of the state space, while retaining the more convenient autonomous form of the problem. Eqn. (33)–(35) are summed:

$$\begin{aligned} \frac{d}{dt} [B + A + M] &= -\frac{F}{V} ([B + A + M] \\ &\quad - [B_f + A_f + M_f]). \end{aligned} \quad (36)$$

This has the form of the classical conservative system $d\theta/dt = -\lambda(\theta - \theta_\lambda)$ which is integrable with the solution $\theta = \theta_\lambda + (\theta_0 - \theta_\lambda)e^{-\lambda t}$. Therefore we can use the integrated form of eqn. (36) to eliminate one state variable:

$$\begin{aligned} [B + A + M] &= [B_f + A_f + M_f] + ([B_0 + A_0 + M_0] \\ &\quad - [B_f + A_f + M_f])e^{-(F/V)t}. \end{aligned} \quad (37)$$

We see that for arbitrary initial conditions the system contains a transient term that approaches zero as $t \rightarrow \infty$, but if we pre-

scribe the initial conditions so that $B + A + M = B_f + A_f + M_f$ this term drops out. Choosing first to eliminate A we can write $A = B_f - B - M$, where for simplicity A and M are absent from the feed stream to the vessel. In the “negligible precursor consumption” approximation we take $B_f - B \approx B_f$, effectively reducing the system to a one-dimensional initial-value problem:

$$\frac{dM}{dt} = k_2(B_f - M) + \phi(M)(B_f - M) - \frac{F}{V} M \quad (38)$$

$$B_0 = B_f, \quad A_0 = A_f = 0, \quad M_0 = M_f = 0. \quad (39)$$

However, we may build up a more informative picture of the state and parameter space by retaining explicitly a planar form of the system. Using eqn. (37) to eliminate B we arrive at

$$\frac{dA}{dt} = k_1(B_f - A - M) - k_2 A - \phi(M)A - \frac{F}{V} A \quad (40)$$

$$\frac{dM}{dt} = k_2 A + \phi(M)A - \frac{F}{V} M \quad (41)$$

$$B_0 = B_f, \quad A_0 = 0, \quad M_0 = 0. \quad (42)$$

With the approximation $B_f - A - M \approx B_f$ eqn. (40)–(42) are equivalent to the dimensionless eqn. (5)–(7) with $\phi(M) = k_3 M^2$. This approximation is physically realistic, yet simplifies the algebra considerably while not changing the qualitative results.

Appendix B: Dimensionless groups

In accordance with traditional practice in dynamical systems analysis the equations in this work are written using dimensionless variable and parameter groups. These free us of the burden of unit dimensions when carrying out algebraic manipulations, and also clear away parameters that are redundant to the bifurcation analysis. The dimensionless groups are defined so that the integrity is retained of physically distinct properties and quantities that are important in defining system behaviour. They are listed in Table 1.

It can be seen from the definitions that μ and r are intrinsic or design parameters, expressing the ratios of the precursor decay rate constant to the autocatalytic rate constant and the

Table 1 Definitions of dimensionless variables and parameters. n is a positive integer exponent that depends on the effective order of the autocatalytic reaction rate: throughout this work $n = 2$

	Dimensionless group	Definition
Eqn. (3) and (4)	x	A/B_0
	y	M/B_0
	b	B/B_0
	τ	$tk_3 B_0^n$
	μ	$k_1/(k_3 B_0^n)$
Eqn. (5)–(7)	r	$k_2/(k_3 B_0^n)$
	x	A/B_f
	y	M/B_f
	b	B/B_f
	τ	$tk_3 B_f^n$
Eqn. (24) and (25)	μ	$k_1/(k_3 B_f^n)$
	r	$k_2/(k_3 B_f^n)$
	f	$F/(Vk_3 B_f^n)$
	x	A/B_0
	y	M/B_0
	b	B/B_0
	τ	$tk_3 B_0^n$
	μ	$k_1/(k_3 B_0^n)$
	r	$k_2/(k_3 B_0^n)$
	η	$k_4/k_3 B_0^n$
	α	$k_5/k_3 B_0^n$

non-catalytic to the autocatalytic rate constants respectively, while f (in the CSTR context at least) is a tunable control or operating parameter. The other tunable quantity is B_0 or B_f , the initial concentration of the precursor, which is incorporated into the definitions of all the variables and parameters (except γ). If it is desired to extract B_0 or B_f as a tunable parameter it is a simple matter to recast the equations appropriately. For example, we can multiply eqn. (5) and (6) by $1/\mu = k_3 B_f^2/k_1 \equiv \beta$ and define $\tau' = tk_1$, $r' = k_2/k_1$ and $f = F/Vk_1$ to obtain the following form of the system:

$$\frac{dx}{d\tau'} = 1 - \beta xy^2 - x(r' + f')$$

$$\frac{dy}{d\tau'} = r'x + \beta xy^2 - f'y.$$

For this analysis we have chosen to work with the dimensionless groups in Table 1, which have both heuristic and practical value, in terms of subsequent algebraic simplicity. The choice of dimensionless groupings does not affect the bifurcation structure of the parameter space.

References

- 1 P. A. Bachmann, P. L. Luisi and J. Lang, *Nature*, 1992, **357**, 57.
- 2 J. Billingham and P. V. Coveney, *J. Chem. Soc., Faraday Trans.*, 1994, **90**(13), 1953.
- 3 P. V. Coveney and J. A. D. Wattis, *Proc. R. Soc. London, Ser. A*, 1996, **452**, 2079.
- 4 T. Buhse, R. Nagarajan, D. Lavabre and J. C. Micheau, *J. Phys. Chem. A*, 1997, **101**, 3910.
- 5 J. B. Maillet, V. Lachet and P. V. Coveney, *Phys. Chem. Chem. Phys.*, 1999, **1**(23), 5277.
- 6 S. J. Marrink, D. P. Tieleman and A. E. Mark, *J. Phys. Chem. B*, 2000, **104**(51), 12165.
- 7 M. Golubitsky and D. G. Schaeffer, *Singularities and Groups in Bifurcation Theory*, Springer-Verlag, New York, 1985, vol. 1.
- 8 M. W. Hirsch and S. Smale, *Differential Equations, Dynamical Systems and Linear Algebra*. Academic Press, New York, 1974.
- 9 C. H. Yang and B. F. Gray, *Trans. Faraday Soc.*, 1969, **65**, 1614.
- 10 R. Ball and B. F. Gray, *Ind. Eng. Chem. Res.*, 1995, **34**, 3726.
- 11 P. Ruoff and R. M. Noyes, *J. Phys. Chem.*, 1985, **89**, 1339.
- 12 P. Strizhak and M. Menzinger, *J. Phys. Chem.*, 1996, **100**(49), 19182.
- 13 R. V. Ball, G. M. Eckert, F. Gutman and D. K. Y. Wong, *Anal. Chem.*, 1994, **66**(7), 1198.
- 14 Amiodarone is an amphiphilic drug used in the treatment of cardiac arrhythmia.
- 15 T. Buhse, V. Pimienta, D. Lavabre and J-C. Micheau, *J. Phys. Chem. A*, 1997, **101**, 5215.
- 16 M. Hirai, T. Takizawa, S. Yabuki, Y. Nakata and K. Hayashi, *Biophys. J.*, 1996, **70**(4), 1761.
- 17 M. Corti, E. Del Favero, E. Digirolamo and A. Raudino, *J. Phys. II France*, 1996, **6**, 1067.
- 18 M. Boretta, L. Cantu, M. Corti and E. Del Favero, *Physica A*, 1997, **236**, 162.
- 19 L. Cantu, M. Corti, E. Del Favero, E. Muller, A. Raudino and S. Sonnino, *Langmuir*, 1999, **15**, 4975.
- 20 L. Cantu, M. Corti, E. Del Favero and A. Raudino, *J. Phys. A*, 2000, **12**, 321.
- 21 *Biological Function of the Gangliosides*, ed. L. Svennerholm, Elsevier, Amsterdam, 1992.
- 22 S. Li, C. J. Clarke, R. B. Lennox and A. Eisenberg, *Colloids Surf. A*, 1998, **133**(3), 191.
- 23 C. J. van Oss, D. R. Absalom, A. L. Grossberg and A. W. Neumann, *Immunol. Commun.*, 1979, **8**(1), 11.
- 24 G. L. Yuen, P. E. Hockberger and J. C. Houk, *Biol. Cyber.*, 1995, **73**(4), 375.
- 25 B. A. Hills, I. B. Masters and J. C. Vance, *Med. Hypoth.*, 1995, **44**(6), 431.
- 26 D. Tyshenko, M. G. Doucet, P. L. Davies and V. K. Walker, *Nat Biotechnol.*, 1997, **15**(9), 887.
- 27 A. D. Haymet, L. G. Ward, M. M. Harding and C. A. Knight, *FEBS Lett.*, 1998, **430**(3), 301.
- 28 E. Porcher and M. Gatto, *J. Theor. Biol.*, 2000, **205**, 283.
- 29 J. J. Tyson, B. Noval, G. M. Odell, C. Chen and C. D. Thron, *Trends Biochem. Sci.*, 1996, **21**, 89.
- 30 U. S. Bhalla and R. Iyengar, *Chaos*, 2001, **11**(1), 221.
- 31 J. E. Ferrell and W. Xiong, *Chaos*, 2001, **11**(1), 227.
- 32 G. Nicolis and I. Prigogine, *Self-Organization in Non-Equilibrium Systems*, Wiley, New York, 1977.
- 33 P. Gray and S. K. Scott, *J. Phys. Chem.*, 1983, **87**(11), 1835.
- 34 J. H. Merkin, D. J. Needham and S. K. Scott, *J. Eng. Math.*, 1987, **21**, 115.
- 35 J. H. Merkin, D. J. Needham and S. K. Scott, *SIAM J. Appl. Math.*, 1987, **47**, 1040.
- 36 S. R. Kay, S. K. Scott and P.-G. Lignola, *Proc. R. Soc. London, Ser. A*, 1987, **409**, 433.
- 37 B. F. Gray, J. H. Merkin and M. J. Roberts, *Dynam. Stabil. Syst.*, 1989, **4**(1), 31.
- 38 P. Gray and S. K. Scott, *Chemical Oscillations and Instabilities*, Clarendon Press, Oxford, 1990.
- 39 Y. A. Chizmadzhew, M. Maestro and F. Mavelli, *Chem. Phys. Lett.*, 1994, **226**, 56.
- 40 J. Billingham, *Q. J. Mech. Appl. Math.*, 2000, **53**(2), 285.
- 41 J. E. Marsden and M. McCracken, *The Hopf Bifurcation and its Applications*, Springer-Verlag, Berlin, 1976.
- 42 D. W. Jordan and P. Smith, *Nonlinear Ordinary Differential Equations*, Clarendon Press, Oxford, 2nd edn., 1987.
- 43 R. Ball, *Proc. R. Soc. London, Ser. A*, 1999, **455**, 141.